Anisotropic Nanocluster Arrays to Diminished Zone: Different regimes of surface deposition in gold nanocolloids

Sanjoy Khawas,[a] and Sunita Srivastava *[a]

[a] *Department of Physics, Indian Institute of Technology Bombay, Powai, India, Maharashtra-400076*

1 Synthesis and characterization

1.1 Materials

Chloroauric acid ($HAuCl_4.3H_2O$) was purchased from Honeywell Fluka. Cetyltrimethylammonium bromide (CTAB), sodium borohydride ($NaBH_4$) and L-ascorbic acid($C_6H_80_6$) were purchased from Spectrochem. Silver nitrate($AgNO_3$), acetone, sulphuric acid and hydrogen peroxide were obtained from Merck's life science.

1.2 Synthesis of monodisperse gold nanorods

Highly monodisperse gold nanorods(AuNR) were synthesized by a seed-mediated growth process[1]. At the initial stage of the synthesis, seed solution was prepared by mixing the CTAB solution(0.2M, 5ml) and gold solution(0.5mM, 5ml) followed by the addition of freshly prepared ice-cold NaBH4 (10mM, 600μL) under vigorous stirring for 2 minutes at 1000rpm. The color of the seed solution turns gray. The seed solution was kept at room temperature for 30minutes before use. Growth solution was prepared by proper addition of gold solution(5mM, 9ml) and silver nitrate solution(0.1M, 112μL) into the CTAB solution and then HCl (1.2M, 112μL) was added into the mixer. Then mild freshly prepared reducing agent ascorbic acid(10mM, 5.5ml) was added under mild stirring(at 800rpm for 10s) after which the blend turned into a colorless solution. Finally, 75μL of seed solution was added to the growth solution and stirred gently for 10s and then kept for particle growth at room temperature for 12hrs. Then the desired volume of growth solution was centrifuged twice at 12000rpm for 15min to remove the excess CTAB and other contaminants. The final suspension was stored in a dark place at room temperature for further use.

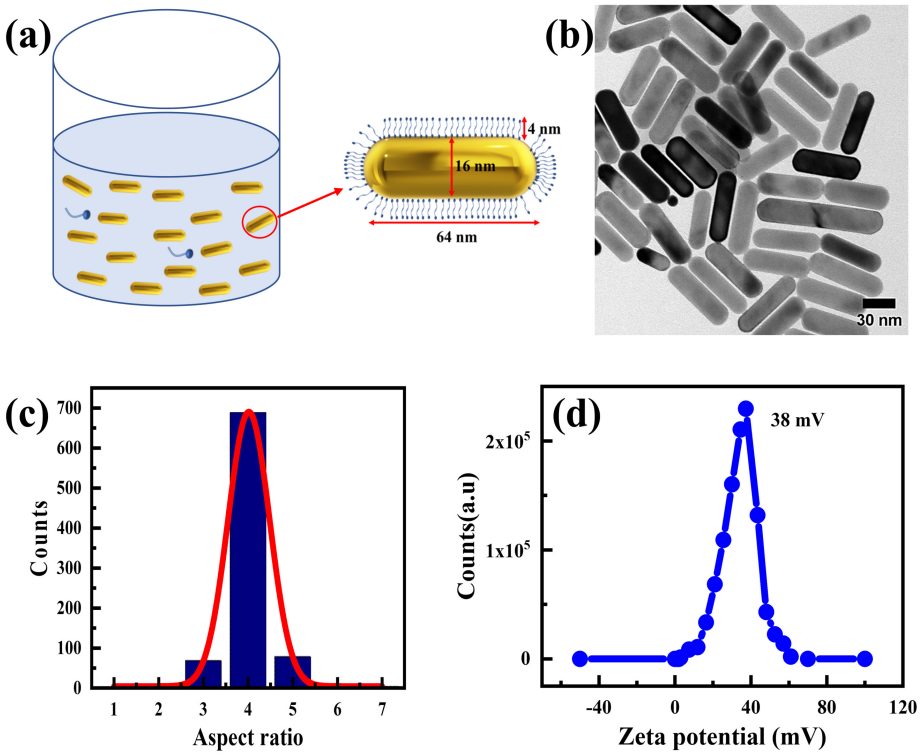

Fig. S1 (a) Schematic of CTAB-AuNR suspension. (b) TEM image of synthesized CTAB-AuNR. (c) Size distribution estimates from TEM images indicating fairly mono disperse gold nanorods. (d) Zeta potential estimate of the CTAB coated AuNR showing positive surface charge and stable dispersion.

1.3 Characterization

The quality of synthesized AuNRs was characterized by UV-visible spectroscopy (Jasco V-730), TEM(JEOL 2100-F) and zetasizer(Nano ZS). The position of longitudinal and transverse resonance peaks is at $750nM$ and $510nM$ respectively. The average length of AuNRs is $63.37 \pm 0.10\ nM$ and the average diameter $16.37 \pm 0.05\ nM$ with a statistical aspect ratio 4.03. The zeta potential of the growth solution is approximately $+46mV$ (Fig. S1).

2 Calculation for interaction potential energy of the ordered AuNR assembly nanostructures

The assembly of AUNRs is primarily assembled into an order structures under the influence of dipole-dipole interaction(U_d), Vanderwaal's interaction(U_{vw}) and depletion interaction(U_{dep}). An estimate of total interaction potential foe side-side AuNRs assembly is given below.

$$U_{total} = U_d + U_{Vw} + U_{dep} \tag{1}$$

$$U_d = -\frac{\mu_1 \mu_2}{4\pi\varepsilon\varepsilon_o d^3} \tag{2}$$

where $= \mu_1 = \mu_2 = 2.4 \times 10^{-25} C.m$, $\varepsilon = 80$ is the relative permittivity and $\varepsilon_o = 8.85 \times 10^{-12} F/m$ is permittivity of the free space. $d = 20nm$ is the separation between nanorods including CTAB layer. The dipole-dipole interaction among the nanorods for the side-side configuration can be approximated as $196 K_B T$.

$$U_{Vw} = -\frac{Alr^{1/2}}{24d^{3/2}} \tag{3}$$

where $A = 4 \times 10^{-19} J$ is the Helmer constant, $l = 63nm$ length of nanorods, $r = 8nm$ is the radius of nanorods. The Vanderwaal's interaction for the side-side configuration can be approximated as $8 K_B T$.

$$U_{dep} = -P_o V_{op} = -n_c RT \times V_{op} \tag{4}$$

where n_c is the micell concentration, R the is universal gas constant and T is temperature and V_{op} is overlap volume. The attractive depletion interaction potential $\approx 3 K_B T$.

3 *In-situ* evaporation kinetics of the drying sessile drop of anisotropic colloidal suspensions

The droplet life span at different stages changes with concentration, as discussed in the paper in details. The variation in the evaporation profile is presented below in normalized time scale (Fig. S2). The relative time scale for various modes of evaporation for the individual AuNRs suspension is tabulated in Table S2. The distinction between the initial droplet diameter and the ring diameter from Table S1, clearly indicates the autophobic effect at lower concentrations and early stage pinning of *TPCL* at higher concentration regime.

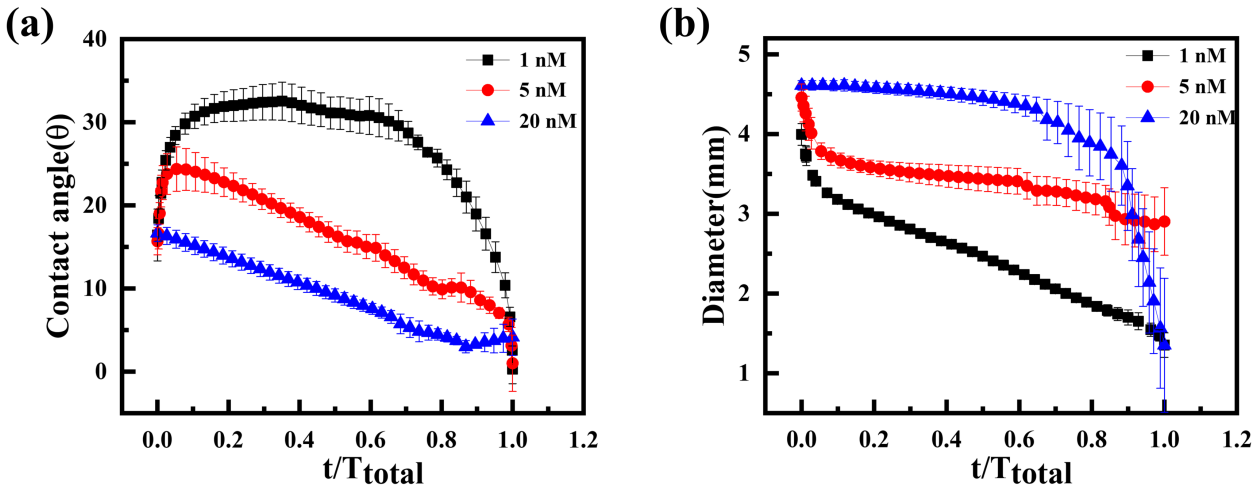

Fig. S2 The *in-situ* drying profile showing (a) contact angle(θ) and (b) diameter vs the normalised droplet evaporation time. Different modes of evaporation can be seen which gradually evolves into a single mode with an increase in particle concentration.

Table 1 Comparsion of droplet diameter immediately after dropcast and ring diameter after complete evaporation of the droplet for different AuNR concentrated suspension.

AuNR concentration(nM)	Droplet diameter(mm)	Ring diameter(mm)	Difference(ΔR in mm)
1	3.95	2.212	1.738
2.5	3.86	2.264	1.596
5	4.39	2.41	1.98
10	3.69	3.496	0.194
20	4.67	4.225	0.445

Table 2 Droplet life span at different mode of evaporation for various AuNR concentration.

AuNR concentration(nM)	Dipinning stage(t_d/T_{total})	CCA(t_{CCA}/T_{total})	Collopse(t_{col}/T_{total})
1	0.1	0.7	0.2
5	0.07	0.84	0.09
20	absent	0.85	0.15

4 Surface properties at varying AuNR/CTAB concentration

The CTAB in the bilayer and residual free CTAB present in the suspension plays a vital role in controlling the pattern morphology. CTAB is a surface-active molecule that reduces the surface tension of the solvent.

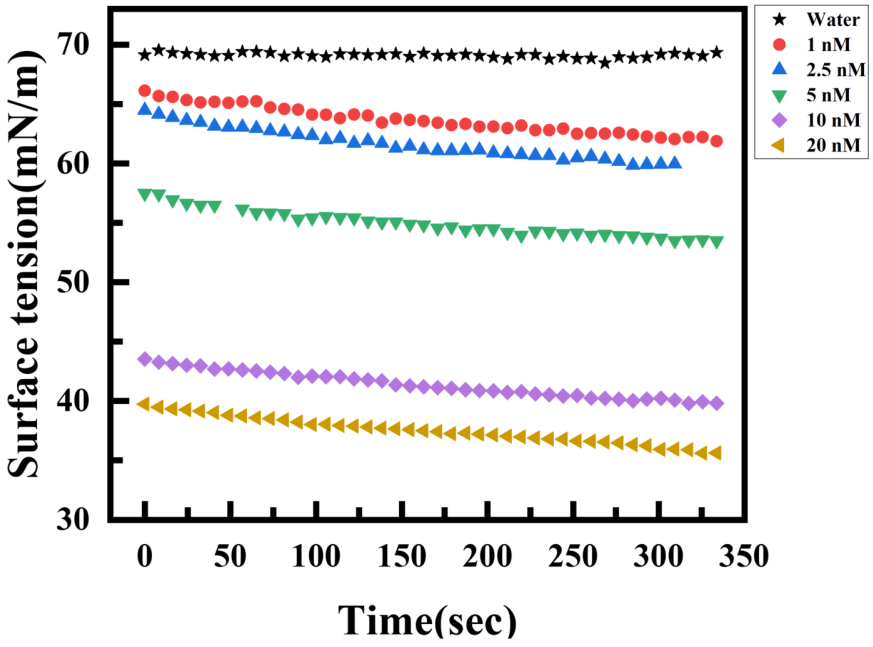

Fig. S3 The estimate of the surface tension values of the AuNR suspension for different concentrations in pendant drop mode. The surface tension at the air-water interface were found to decrease with increase in AuNR concentration.

Non-uniform accumulation of CTAB during evaporation may alternate the regular fluid dynamics across the droplet, resulting in variation in the deposited morphology. The CTAB concentration in the suspension increases with the nanorods concentration (Fig.S3). The surface tension of the different concentrated suspensions was measured using a contact angle meter in pendant drop mode for the initial $350s$ when the CTAB and nanorods are distributed homogeneously across the pendant drop. The surface tension of $1nM$ AuNR suspension $\approx$ 66 mN/m while it decreased to 40 mN/m for the $20nM$ suspension commencing the higher CTAB concentration in $20nM$ AuNR suspension.

5 Surface morphologies at varying nanoparticle concentration

The middle region of the coffee ring contains scatter nanoclusters of AuNR. But the number of cluster significantly increases at higher concentrations because of a larger fraction of rods captured by the interface which later directly transferred to the substrate. The stronger inward Marangoni flow also plays

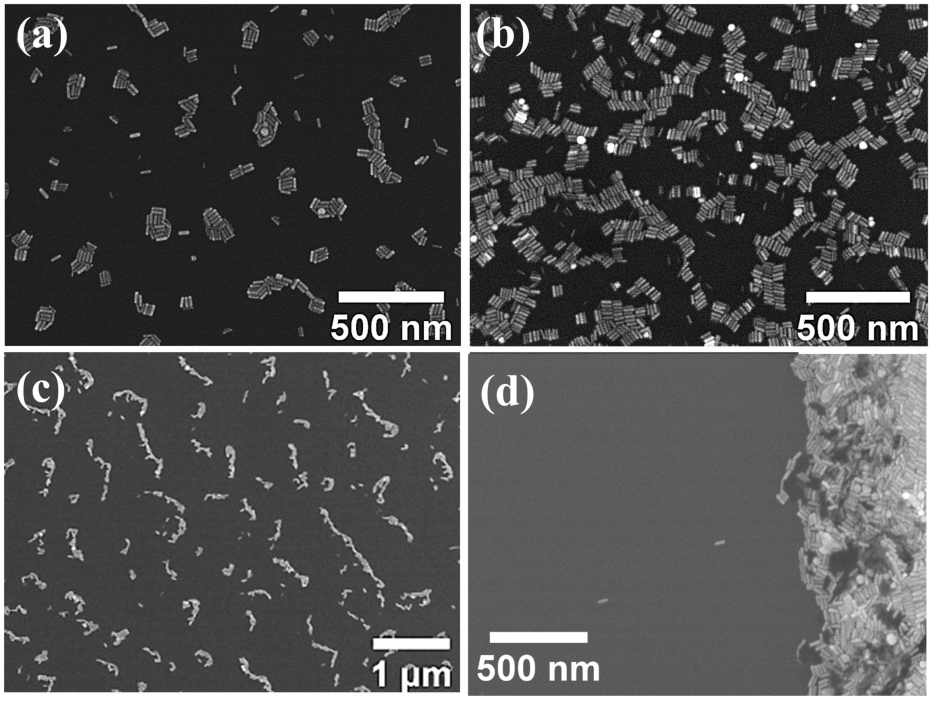

Fig. S4 (a-b) SEM images showing the morphology in *region* 4 of the dried particulate at $1nM$ and $20nM$ respectively. (c-d) The morphology outside the coffee-ring deposit, *region* 1, for $1nM$ and $20nM$ respectively. The nanocluster array deposition can be seen for $1nM$ sample, whereas *region* 1 lacks the same for $20nM$ AuNR suspension.

an important role in pulling the AuNR towards the droplet center. For the same reason, large no. of nanoclusters at the middle of the 20 *nM* deposition observed compared to 1 *nM* deposition as shown in Fig. S4(a,b). The outer nanoclusters region appears at lower concentrations due to autophobe-induced depinning of the *TPCL* which is shown Fig. S4(c) for 1 *nM* suspension, while it disappears at a higher concentration as shown in Fig. S4(d) for 20 *nM* suspension. The particle arrangement within the coffee

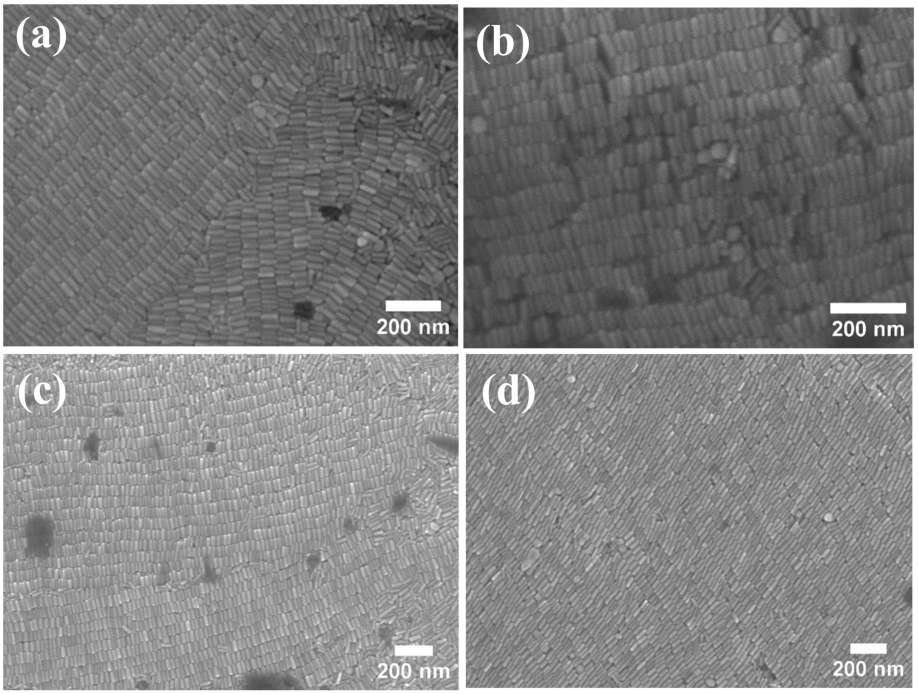

Fig. S5 The internal nanoscale arrangements of AuNR within the coffee-ring showing smectic ordering at varying AuNR concentrations (a) $1nM$, (b)$2.5nM$, (c) $10nM$ and (d) $20nM$. The ordering improves with an increase in particle concentration.

ring for various concentrations shown in Fig. S5. The area of the ordered domains increases with AuNR concentrations as reported in our previous work[2].

To identify the role of CTAB on the final deposition pattern, drying experiments were performed with 1 *nM* AuNR suspension with additional CTAB of different concentrations. Different CTAB concentrated AuNR suspensions were made by adding the additional CTAB e.g. $0.1mM$, $0.4mM$, $0.5\ mM$ and $1mM$ in 1 *nM* AuNR suspension. The variation in the width of the ring for various CTAB concentrations is shown in Fig. S6. The width of the ring from $0.1mM$ suspension is a compact one, while for $0.4mM$ and $0.5mM$, the width is heterogeneous and tends to thin towards the inner side of the ring. For $1mM$ CTAB added suspension, diminished ring is formed at the inner side which is two or three layer thick, marked as region $2b$ in Fig. S6(d) while region $2a$ is thicker with 10-12 AuNR layer. The thinning of ring width towards the inner side of the ring reported previously due to the thermocapillary Marangoni flow[3,4]. In our case, a local CTAB-dense region is formed near *TPCL* during evaporation which induces an inward solutocapilliary Marangoni flow. A higher fraction of CTAB in the suspension persuades a strong inward flow which tends to carry the particles from *TPCL* to the apex of the droplet and form a diminished ring at the inner side of the ring.

The presence of a larger fraction of CTAB in higher concentrated suspension affects both the ring width

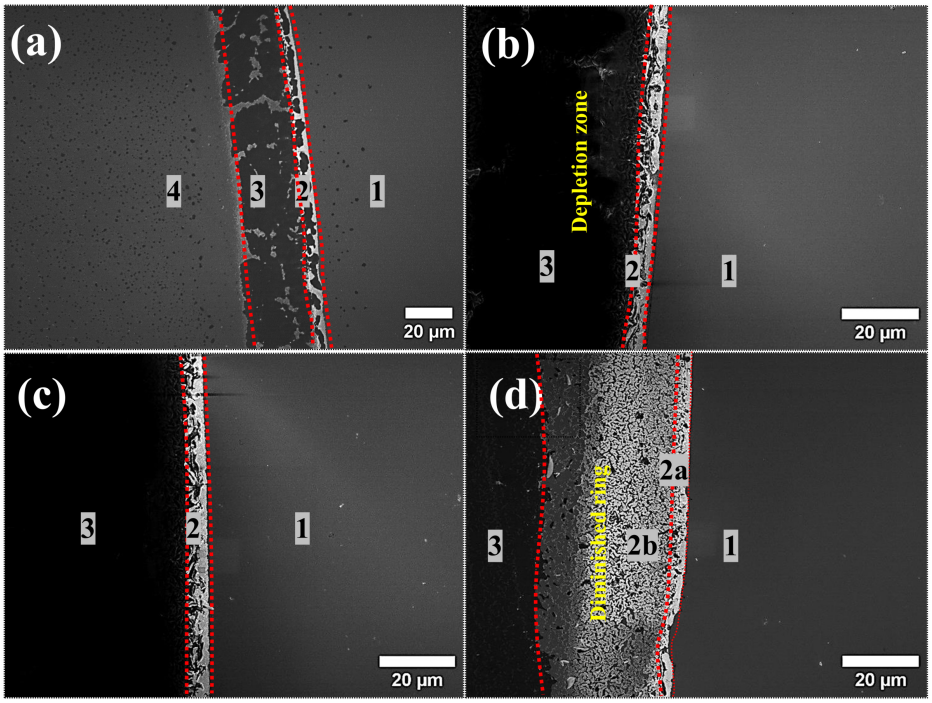

Fig. S6 (a-d) SEM images for 1nM AuNR suspension with added $0.1mM, 0.4mM, 0.5mM$ and $1mM$ concentration of CTAB molecules, respectively. The variation in surface morphology due to inward solutal Marangoni flow induced by larger amount of CTAB at higher AuNRs concentration is evident.

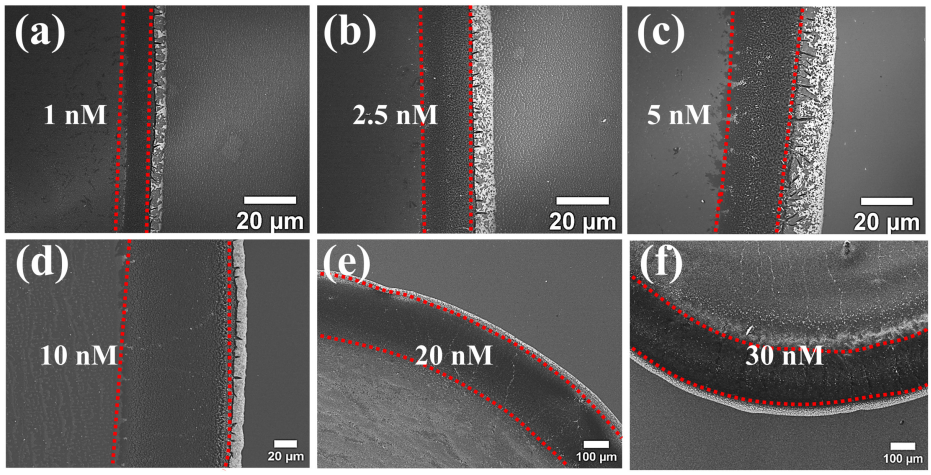

Fig. S7 Surface morphology of the dried particulate using SEM at indicated AuNR concentration. (a-c) shows the enhancement in the depletion zone with nanorods cocnetration. (d-f) The depletion zone width saturates at higher AuNRs concentration (beyond 10 nM). The scale bars are marked alongside each image.

and depletion zone in the inner vicinity of the coffee ring. Intially depletion zone get enhanced and then almost saturates at higher AuNR concentration Fig. S7. Beyond a certain AuNR concentration($\geq 30nM$), depletion zone morphology changes significantly Fig. S8. We examined the width as well as depletion zone of the deposited pattern from different concentrated AuNR suspensions using a Stylus Profilometer.

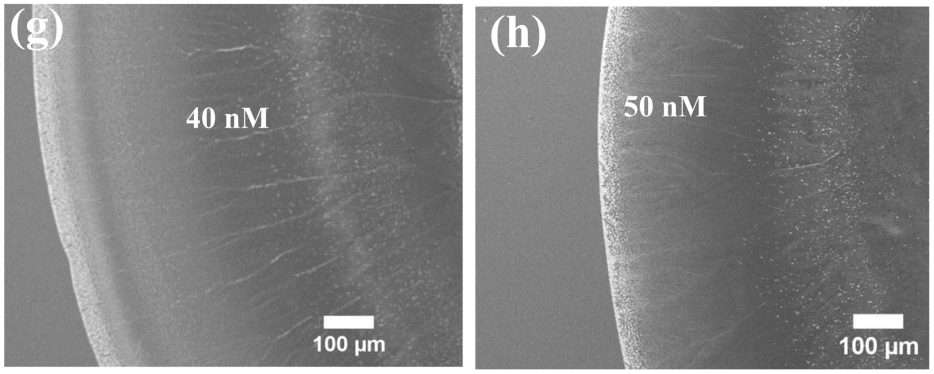

Fig. S8 Surface morphology using SEM at AuNR concentration of 40 nM (g) and 50nM (h). Significant change in surface morphology were observed with formation of uniform deposition for these samples.

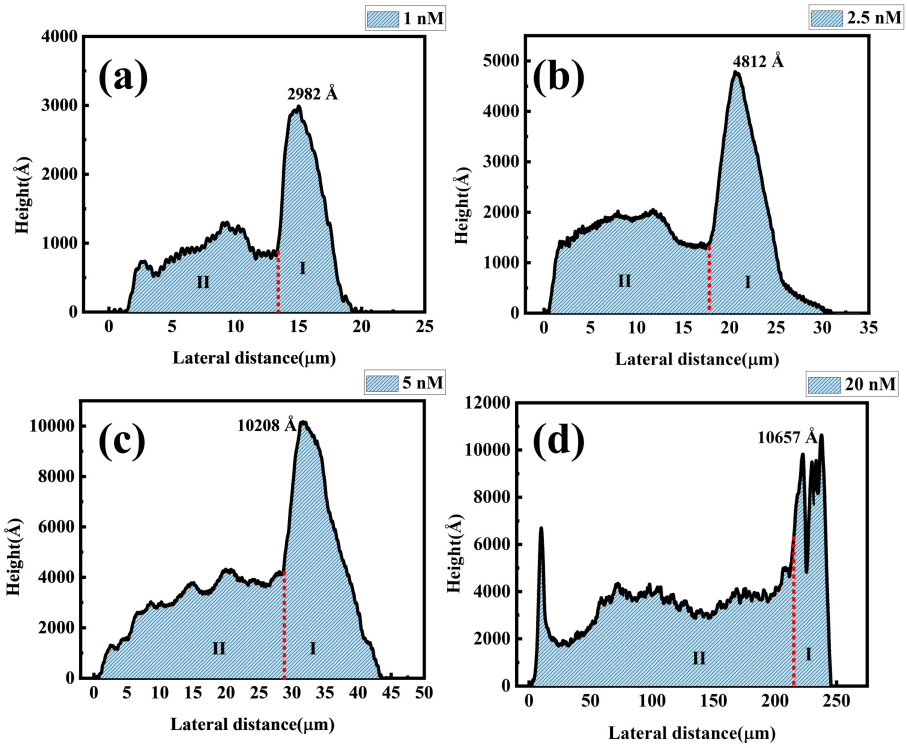

Fig. S9 (a)-(d) The profilometer data to estimate the ring width(I) and depletion zone width(II) at varying nanoparticle concentration, as indicated alongside each graph.

Both the ring width and depletion zone, marked as I and II in Fig. S9 show an incremental tendency with AuNR concentration consistent with the SEM analysis. The height of the ring and depletion zone (region II) also gets increased with AuNR concentration, indicating the more significant fraction of AuNR and CTAB deposition in the I and II, respectively at higher AuNR concentration.

6 *In-situ* video of the drying droplet using confocal microscope

6.1 Movie 1 (Avaliable online)

Shows the various phases of *TPCL* motion during the evaporation for 1nM AuNR suspension. Initial receding of *TPCL* due to autophobic effect leads to outer nanocluster region. The pinning stage of *TPCL* promotes coffee ring formation. The *TPCL* receeding at the final stage of drying leads to the appearance of the depletion zone and the central nanocluster region.

6.2 Movie 2 (Avaliable online)

Shows the various phases of *TPCL* motion during the evaporation for 20nM AuNR suspension. Initial strong pinning of the *TPCL* is correlated with the absence of of the outer nanocluster deposition in region 1. At the collapse state, comparatively early stage receding of the *TPCL* for a longer period of time leads to the wider depletion zone at 20nM AuNR suspension.

Notes and references

1 B. Nikoobakht and M. A. El-Sayed, *Chemistry of Materials*, 2003, **15**, 1957–1962.

2 A. Zaibudeen, S. Khawas and S. Srivastava, *Colloid and Interface Science Communications*, 2021, **44**, 100492.

3 N. D. Patil, P. G. Bange, R. Bhardwaj and A. Sharma, *Langmuir*, 2016, **32**, 11958–11972.

4 S. Chatterjee, M. Kumar, J. S. Murallidharan and R. Bhardwaj, *Langmuir*, 2020, **36**, 8407–8421.